



University of  
Massachusetts  
Amherst

## Avoiding infrared catastrophes in trapped Bose-Einstein condensates

Item Type	article;article
Authors	Kevrekidis, PG;Theocharis, G;Frantzeskakis, DJ;Trombettoni, A
Download date	2024-11-13 04:48:45
Link to Item	<a href="https://hdl.handle.net/20.500.14394/34977">https://hdl.handle.net/20.500.14394/34977</a>

# Avoiding Infrared Catastrophes in Trapped Bose-Einstein Condensates

P.G. Kevrekidis<sup>1</sup>, G. Theocharis<sup>2</sup>, D.J. Frantzeskakis<sup>2</sup>, and A. Trombettoni<sup>3</sup>

<sup>1</sup> *Department of Mathematics and Statistics, University of Massachusetts, Amherst MA 01003-4515, USA*

<sup>2</sup> *Department of Physics, University of Athens, Panepistimiopolis, Zografos, Athens 15784, Greece*

<sup>3</sup> *Istituto Nazionale per la Fisica della Materia and Dipartimento di Fisica, Universita' di Parma, parco Area delle Scienze 7A, I-43100 Parma, Italy*

This paper is concerned with the long wavelength instabilities (infrared catastrophes) occurring in Bose-Einstein condensates (BECs). We examine the modulational instability in “cigar-shaped” (1D) attractive BECs and the transverse instability of dark solitons in “pancake” (2D) repulsive BECs. We suggest mechanisms, and give explicit estimates, on how to “engineer” the trapping conditions of the condensate to avoid such instabilities: the main result being that a tight enough trapping potential suppresses the instabilities present in the homogeneous limit. We compare the obtained estimates with numerical results and we highlight the relevant regimes of dynamical behavior.

## I. INTRODUCTION AND SETUP

Infrared catastrophes, or long-wavelength instabilities (LWI) as they are otherwise known, are ubiquitous in physical phenomena. From Magneto-Hydro-Dynamics [1] to chemical models [2], and from quantum systems [3] to fluid mechanics [4], polymer physics [5] and plasmas [6], large scale modulations may destabilize the system of interest. On the other hand, many of these instabilities (and their thresholds) have been quantified in the context of nonlinear models.

In the past few years, another context that can be accurately modeled by nonlinear partial differential equations that are known to possess LWI, has become experimentally tractable. This setting is, in particular, the one of Bose-Einstein condensates (BECs) [7] whose experimental realization has led to an explosion of interest in the field of atomic matter waves and of nonlinear excitations in them. Such nonlinear waves have been recently experimentally generated in BECs, namely dark [8] and bright [9,10] solitons. Also, two dimensional excitations, such as vortices [11] and lattice patterns thereof [12] have also been obtained experimentally, while other nonlinear waves, such as Faraday waves [13], ring solitons and vortex necklaces [14] have been theoretically predicted. It is worth noting here that the nature of Bose-Einstein nonlinear matter waves depends crucially on the type of the interatomic interactions: dark (bright) solitons can be created in BECs with repulsive (attractive) interatomic interactions, resulting from positive (negative) scattering length.

In the present work, our scope is to re-examine the LWI in the context of Bose-Einstein condensates and exploit the consequences on the LWI of the inhomogeneity induced by the trapping potential. It is well-known [7] in this setting that the condensates are formed under appropriate confining conditions that typically consist of magnetic traps modeled by parabolic potentials. Our scope is then two-fold. On the one hand, we aim at illustrating the potential for the instabilities and at examining their dynamical development when they exist. On the other hand, the magnetic confinement provides an additional “trapping” length scale to the problem whose *competition* with the instability length scale may disallow the dynamical manifestation of the LWI. In this way, we will propose how to *engineer* trapping conditions so as to prevent unstable dynamical evolution.

We will examine two benchmark examples of long-wavelength instabilities in BECs: the modulational instability occurring in attractive, one-dimensional (1D) BECs and giving rise to the formation of bright matter-wave solitons, and the transverse (“snaking”) instability of dark soliton stripes formed in repulsive two-dimensional (2D) BECs. It should be noted here that the genuinely three-dimensional (3D) condensate can be considered as approximately 1D if the nonlinear inter-atomic interaction is weak relative to the trapping potential force in the transverse directions; then, the transverse size of the condensates is much smaller than their length, i.e., the BEC is “cigar-shaped” and can be effectively described by 1D models [15,16]. Similarly, if the transverse confinement is strong along one direction and weak along the others, then for this “pancake-shaped” BEC, 2D model equations are relevant [17].

Close to zero temperature, it is well-known that the 3D Gross-Pitaevskii (GP) equation [7] accurately captures the dynamics of the condensate. For cigar-shaped BECs, the model equation is effectively 1D and can be expressed in the following dimensionless form,

$$i \frac{\partial u}{\partial t} = -\frac{1}{2} \frac{\partial^2 u}{\partial x^2} + \alpha |u|^2 u + V(x)u, \quad (1)$$

where  $u$  is the macroscopic wave function (normalized to 1), and  $\alpha = a/|a| = \pm 1$  is the renormalized scattering length, which is positive (negative) for repulsive (attractive) condensates. In this equation,  $t$  and  $x$  are respectively measured

in units of  $9/16\epsilon^2\omega_\perp$  and  $3a_\perp/4\epsilon$ , where  $\omega_\perp$  is the confining frequency in the transverse direction,  $a_\perp = \sqrt{\hbar/m\omega_\perp}$  is the transverse harmonic-oscillator length and  $\epsilon \equiv N|a|/a_\perp$  is a small dimensionless parameter,  $N$  being the total number of atoms [16]. Finally,

$$V(x) = \frac{\Omega^2}{2}x^2 \quad (2)$$

where  $\Omega = (9/16\epsilon^2) \cdot (\omega_x/\omega_\perp)$  is the frequency of the magnetic trap potential  $V$  in our dimensionless units, and  $\omega_x$  is the axial confining frequency. Similarly the 2D model for the pancake-shaped condensate assumes the form:

$$i\frac{\partial u}{\partial t} = -\frac{1}{2}\Delta u + \alpha|u|^2u + V(r)u \quad (3)$$

where now the role of the axial frequency/spatial variable is played by the radial one ( $r \equiv \sqrt{x^2 + y^2}$ ) and the normalized variables are connected to the dimensional ones similarly to the 1D case, but with the role of  $\omega_x$  ( $\omega_\perp$ ) now played by  $\omega_\perp$  ( $\omega_z$ ).

We structure our presentation as follows: in Section II we study the suppression of the modulational instability for 1D cigar-shaped BECs in presence of a tight confining magnetic potential, while in Section III we investigate the transverse instability for 2D trapped BECs. In both cases we provide a criterion (in terms of the trap parameters) giving the conditions under which LWI can be avoided. Section IV is devoted to our concluding remarks.

## II. MODULATIONAL INSTABILITY

It is well-known (see, e.g., the recent work [18] and references therein) that, in the absence of external potential, the continuous-wave (cw) solution  $u = u_0 \exp(-i\alpha u_0^2 t)$  of amplitude  $u_0$ , of Eq. (1) becomes modulationally unstable when perturbations of wavenumber  $k < k_{cr} \equiv 2|\alpha|^{1/2}u_0$  are imposed. This can be equivalently interpreted as follows: when length scales

$$\lambda > \lambda_{cr} \equiv \frac{\pi}{u_0\sqrt{|\alpha|}} \quad (4)$$

become “available” to the system, then the modulation over these scales leads the solution to instability.

However, in the presence of the magnetic trap, there is a characteristic scale set by the trap, namely the BEC axial size,  $\lambda_{BEC}$ , which depends on the trapping frequency  $\Omega$ . When  $\lambda_{BEC} < \lambda_{cr}$  suppression of the modulational instability is expected. To estimate  $\lambda_{BEC}$  in a specific setup, we will examine a protocol relevant to the recent experiments conducted by the Rice [9] and Paris [10] groups, which has stimulated a considerable amount of theoretical attention [19]. In particular, we start with a 1D repulsive condensate, whose ground state wavefunction is approximately in the so-called Thomas-Fermi (TF) regime [7], and subsequently change the interaction into an attractive one. This is experimentally achieved using the so-called Feshbach resonance: an external magnetic field is used to modify the scattering length of the interatomic interactions [20]. In our example, we use as initial condition the ground state of Eq. (1) with  $\alpha = 1$ , which is in the TF approximation  $|u|^2 \approx \mu - V(x)$ ; then at  $t = 0$  we change the sign of the scattering length, i.e., we set  $\alpha = -1$ . Therefore in this situation  $\lambda_{BEC} \approx 2\sqrt{2\mu}/\Omega$ . From the normalization condition  $\int dx|u|^2 = 1$  one gets

$$\mu = \left( \frac{3\Omega}{4\sqrt{2}} \right)^{2/3}. \quad (5)$$

The condition for the suppression of the modulational instability  $\lambda_{BEC} < \lambda_{cr}$  [where  $\lambda_{cr}$  is given by Eq. (4)] gives  $\Omega > 2^{3/2}(|\alpha|\mu)^{1/2}u_0/\pi$ . In this context, the amplitude  $u_0$  in Eq. (6) can be well approximated as  $u_0 \approx \sqrt{\mu}$ , since the TF approximation is most accurate close to the center of the condensate. Therefore if  $\Omega > \Omega_{cr}$ , where

$$\Omega_{cr} = \frac{9}{\sqrt{2}\pi^3} \approx 0.2, \quad (6)$$

then the trapping conditions are “engineered” in such a way that the modulational instability cannot manifest itself: for a tight enough trapping potential the modulational instability does not occur. This is one of the key aims of this paper, namely to quantitatively highlight how the infrared catastrophes can be avoided in the presence of sufficiently “tight” trapping of the condensate. We remark that if one evaluates  $\lambda_{BEC}$  by using for the ground state of Eq. (1)

(with  $\alpha = 1$ ) a gaussian with variationally determined width, one has an estimate of  $\Omega_{cr}$  in good agreement with Eq. (6). We also notice that the critical length  $\lambda_{cr}$  is a few healing lengths  $\xi$ : indeed, when the density grows from 0 to  $u_0^2$  within a distance  $\xi$ , the quantum pressure and interaction energy terms are equal when  $1/(2\xi^2) \approx u_0^2$ , which means that  $\xi \approx (\sqrt{2}u_0)^{-1}$  and therefore  $\lambda_{cr} \approx \pi\sqrt{2}\xi = 4.44\xi$ .

Typical experimental values for a  $^7\text{Li}$  BEC are  $\omega_x = 2\pi \times 5\text{Hz}$ ,  $\omega_\perp = 2\pi \times 500\text{Hz}$ ,  $a = -3a_0$  and  $N \approx 10^3$ ; these yield  $\epsilon \sim 0.1$  and  $\Omega \sim 0.5$ , which should be a sufficiently large value to avoid the emergence of the modulational instability.

We tested this prediction by means of direct numerical simulations shown in Fig. 1. The panels (a), (b), (c) show respectively the case of  $\Omega = 0.3, 0.1$ , and  $0.02$ . It is seen that the supercritical, ‘‘tight’’ trap  $\Omega = 0.3$  does not allow the development of the instability for the condensate [Fig. 1 (a)]. The only consequence of the change of the sign of the scattering length is the excitation of an internal mode of the condensate, due to the fact that the TF cloud is not the ground-state for  $\alpha = -1$ . This results in nearly periodic oscillations of the width of the wavefunction  $W = [\int x^2 |u|^2 dx - (\int x |u|^2)]^{1/2}$ , which we monitor as a diagnostic in our numerical examples. For  $\Omega = 0.1$  [Fig. 1 (b)], the width oscillations are no longer periodic: the result of the modulational instability can be clearly discerned in the addition of an extra frequency to the motion of the condensate for subcritical trapping. We have identified this to be a rather smooth transition, becoming more pronounced close to the theoretically predicted critical point of  $\Omega \approx 0.2$ . We have also examined the development of the instability for weaker trapping conditions [ $\Omega = 0.02$ , see Figs. 1 (c), (d)]. Then an additional frequency emerges, as the condensate is now cleaved in two pieces during the time evolution [see Fig. 1 (d)]. For even weaker trappings, we found that the larger the ratio of  $\lambda_{BEC}/\lambda_{cr}$ , the more frequencies appear in the condensate density evolution, rendering it increasingly chaotic. Hence, we have demonstrated that a cascade of frequencies arises in the BEC dynamics due to the modulational instability and subsequent higher resonances that allow the breakup of the condensate and make its motion less regular. This mechanism should clearly be experimentally detectable; in fact we surmise that the observation of a single matter-wave bright soliton [10], rather than a soliton train [9], is due to the fact that  $\lambda_{BEC}$  was smaller in the former case, as the number of atoms was an order of magnitude fewer in the Paris experiment, while the ratio of the trapping frequencies was approximately the same.

### III. TRANSVERSE INSTABILITY

One of the infrared catastrophes that occur in two spatial dimensions is the transverse instability of dark-soliton stripes in repulsive ( $\alpha > 0$ ) BECs. As a result, a dark-soliton undergoes a transverse snake deformation [21], causing the nodal plane to decay into vortex pairs. This instability has been examined in the context of BECs in [22], and the Bogoliubov spectrum of the dark soliton has been obtained; in this context, the relevant imaginary modes were identified to transfer the energy of the condensate to collective excitations parallel to the nodal plane destroying the configuration. However, as is highlighted in [23], ‘‘the explicit connection between the existence of imaginary excitations and a dynamical snake instability remains unclear’’. Our scope here is to illustrate the criterion for the transverse instability and to test it against direct numerical simulations, exposing the possible dynamical scenarios and quantifying their dependence on the trapping parameters.

In the absence of the potential, the transverse instability occurs for perturbation wavenumbers

$$k < k_{cr} \equiv \left[ 2\sqrt{\sin^2 \phi + u_0^{-2} \sin \phi + u_0^{-4}} - (2 \sin \phi + u_0^{-2}) \right]^{1/2}, \quad (7)$$

where  $\sin \phi$  is the dark-soliton velocity [21] and  $u_0$  is the amplitude of the homogeneous background, connected with the chemical potential through  $u_0^2 = \mu$  similarly to the previous (1D) setting. In the case of stationary (black) solitons, of interest here,  $\sin \phi = 0$ , hence  $k_{cr} = u_0^{-1}$ . On the other hand, for  $V(r) = \Omega^2 r^2/2$ , a similar calculation as for the 1D problem yields the characteristic length scale of the BEC (i.e., the diameter of the TF cloud) as  $\lambda_{BEC} \approx 2\sqrt{2\mu}/\Omega$ . Then, the criterion for the suppression of the transverse instability is that the scale of the BEC is shorter than the minimal one for the instability. The corresponding condition reads

$$\Omega > \frac{\sqrt{2\mu}}{\pi u_0}. \quad (8)$$

To obtain the minimum value of  $\Omega$  we need to know how  $\mu$  is connected with  $u_0$ . As a first guess, in the absence of the dark soliton, one can assume  $u_0^2 \approx \mu$  (close to the center of the BEC), which yields  $\Omega > \sqrt{2}/\pi = 0.45$ . Hence, stronger trapping should ‘‘drown’’ the transverse instability and preserve dark soliton stripes on top of the Thomas-Fermi cloud (i.e., stable ‘‘dipole’’ solutions). Note that in terms of real physical units, the above mentioned critical value of  $\Omega$  may

correspond, e.g., to a weakly interacting  $^{87}\text{Rb}$  pancake condensate, containing  $\approx 10^3$  atoms, confined in a trap with  $\omega_r = 2\pi \times 5\text{Hz}$  and  $\omega_z = 2\pi \times 50\text{Hz}$ .

We have numerically tested this condition, finding it to be an *overestimate* of the critical trapping frequency for the transverse instability, which is  $\Omega_{cr} \approx 0.31$ . This result shows that the numerically found Fig. 2 shows a dynamical evolution example of the dipolar solution, initialized with a  $\tanh(y)$  imposed on the TF cloud, for  $\Omega = 0.35$  (left) and  $\Omega = 0.15$  (right). Both snapshots show the contour plot of the square modulus of the wave function at  $t = 1000$  (left) and  $t = 200$  (right). Clearly, in the former case the transverse instability is suppressed, while in the latter a vortex pair has been formed demonstrating the dynamical instability of the configuration. We have monitored the asymptotic, long time evolution of the dipole and have observed the following interesting phenomenology: for  $0.18 \lesssim \Omega \lesssim 0.31$ , while the stripe is dynamically unstable, there is not sufficient space for the instability-induced vortices to fully develop; as a result, after their formation, they subsequently recombine and disappear. This behavior is shown in Fig. 3 (for  $\Omega = 0.2$ ): the two vortices formed are shown at  $t = 190$  (left panel), while at  $t = 210$  they recombine to form a transient dark stripe (right panel). This configuration is unstable and it subsequently breaks up to a new vortex pair (not shown here), which eventually recombines at longer times ( $t \approx 400$ ). It is interesting to note that as, in the present case, the available size of the condensate is of the order of a few healing lengths  $\xi$  (in our units,  $\xi = 1/\sqrt{2}$ ), the two vortices formed hardly fit the condensate size (recall that the vortex core is of order of  $\xi$  [24]). This is a possible qualitative explanation of this recombination, whose origin is the competition of the length scales available in the BEC. Finally, it should be noted that for  $\Omega \lesssim 0.18$ , the vortices will survive in the asymptotic evolution of the system, and naturally the weaker the trapping the larger the number of “engulfed” vortices generated due to the stripe breakup.

A question that naturally arises in the results above concerns the disparity between the critical point theoretical estimate for the transverse instability and the corresponding numerical finding. We believe that the disparity is justified by the fact that the theoretical stability analysis of [21] is performed for the infinite homogeneous medium (the dark-soliton pedestal), in the absence of a magnetic trap. In the presence of the trap on the one hand, the background is inhomogeneous, while, on the other hand, for tight traps resulting in small condensate sizes, the presence of the dark soliton at the BEC center, significantly modifies the maximum density. Thus, one should expect that the relation  $u_0^2 = \mu$  should be modified as  $\delta u_0^2 = \mu$ , where the “rescaling” factor  $\delta < 1$ . Based on the results of the numerical simulations (see Figs. 2-3) we have observed that embedding the dark soliton in the BEC center reduces the maximum density of the TF cloud to the half of its initial value. This suggests that  $\delta = 1/2$ , which, according to Eq. (8), leads to a new value for  $\Omega$  minimum, i.e.,  $\Omega = 1/\pi \approx 0.318$ . This modified criterion for the suppression of the transverse instability, namely  $\Omega > 0.318$  is in very good agreement with the above mentioned numerically found condition  $\Omega > 0.31$ .

#### IV. CONCLUSIONS

We have examined case examples of long wavelength instabilities in Bose-Einstein condensates. We have revisited the modulational instability in quasi-1D, cigar-shaped BECs, and the transverse instability in quasi-2D, pancake-shaped BECs. We have advocated that trapping conditions can be engineered to avoid or induce such instabilities at will. Using the length scale competition of the entrainment due to trapping and of critical instability wavelength, we have given explicit estimates for critical values of the trapping frequency beyond which the instabilities will be absent. We have tested these criteria in both cases and have found good agreement with the numerical results in the 1D case. In the 2D setting, we have explained the overestimation of the critical point, on the basis of the homogeneous background assumed in the theoretical estimate, as well as the modification of the value of the maximum density of the condensate due to the presence of the dark soliton. Our results demonstrate how to engineer the trapping conditions, in order to achieve supercritical regimes, devoid of long wavelength instabilities. On the other hand, for the subcritical regimes, we have illustrated the relevant phenomenology through direct numerical simulations and the cascade that leads to the instability and eventual destruction of the original coherent structure. Such results can be particularly useful in quantifying the selection of external conditions so as to achieve or avoid a given experimental outcome.

This work was supported by the Eppley Foundation and NSF-DMS-0204585 (PGK), the “A.S. Onasis” Public Benefit Foundation (GT) and the Special Research Account of the University of Athens (GT, DJF), and by M.I.U.R. through grant No. 2001028294 (AT).

- [1] V.P. Lakhin and V.D. Levchenko, Plasma Phys. Rep. **29** 328 (2003).  
[2] T.K. Callahan and E. Knobloch, Phys. Rev. E **64**, 036214 (2001); L.Q. Zhou and Q. Ouyang, Phys. Rev. Lett. **85**, 1650 (2000).  
[3] R.K. Moudgil, J. Phys.: Cond. Mat. **12**, 1781 (2000); J.A. Holyst and L.A. Turski, Phys. Rev. A **45**, 6180 (1992).  
[4] W. Boos and A. Thess, Phys. Fluids **11**, 1484 (1999); M. Lee *et al.*, Phys. Rev. Lett. **76**, 2702 (1996).  
[5] Y. Shiwa, Phys. Lett. A **228**, 279 (1997).  
[6] S.P. Gary, Plasma Phys. Contr. F. **15**, 399 (1973); R. Bingham, Phys. Fluids **7**, 1001 (1965).  
[7] L.P. Pitaevskii and S. Stringari, *Bose-Einstein Condensation*, (Oxford University Press, Oxford, 2003).  
[8] S. Burger *et al.*, Phys. Rev. Lett. **83**, 5198 (1999); J. Denschlag *et al.*, Science **287**, 97 (2000); B.P. Anderson *et al.*, Phys. Rev. Lett. **86**, 2926 (2001).  
[9] K.E. Strecker *et al.*, Nature **417**, 150 (2002); K.E. Strecker *et al.*, New. J. Phys. **5**, 73 (2003).  
[10] L. Khaykovich *et al.*, Science **296**, 1290 (2002).  
[11] M.R. Matthews *et al.*, Phys. Rev. Lett. **83**, 2498 (1999); K.W. Madison *et al.* Phys. Rev. Lett. **84**, 806 (2000); S. Inouye *et al.*, Phys. Rev. Lett. **87**, 080402 (2001).  
[12] J.R. Abo-Shaeer *et al.*, Science **292**, 476 (2001); J.R. Abo-Shaeer, C. Raman, and W. Ketterle, Phys. Rev. Lett. **88**, 070409 (2002); P. Engels *et al.*, Phys. Rev. Lett. **89**, 100403 (2002).  
[13] K. Staliunas, S. Longhi, and G. J. de Valca'rcel, Phys. Rev. Lett. **89**, 210406 (2002).  
[14] G. Theocharis *et al.*, Phys. Rev. Lett. **90**, 120403 (2003).  
[15] V.M. Pérez-García, H. Michinel, and H. Herrero, Phys. Rev. A **57**, 3837 (1998); Yu.S. Kivshar, T.J. Alexander, and S.K. Turitsyn, Phys. Lett. A **278**, 225 (2001).  
[16] F.Kh. Abdullaev *et al.*, Phys. Rev. Lett. **90**, 230402 (2003).  
[17] L. Salasnich, A. Parola, and L. Reatto, Phys. Rev. A **65**, 043614 (2002).  
[18] G. Theocharis *et al.*, Phys. Rev. A **67**, 063610 (2003).  
[19] U. Al Khawaja *et al.*, Phys. Rev. Lett. **89**, 200404 (2002); L.D. Carr and J. Brand, Phys. Rev. Lett. **92**, 040401 (2004); L. Salasnich, A. Parola, and L. Reatto, Phys. Rev. Lett. **91**, 080405 (2003).  
[20] S. Inouye *et al.*, Nature **392**, 151 (1998); E.A. Donley *et al.*, Nature **412**, 295 (2001).  
[21] Yu.S. Kivshar and B. Luther-Davies, Phys. Rep. **298**, 81 (1998).  
[22] A.E. Muryshev *et al.*, Phys. Rev. A **60**, R2665 (1999); P.O. Fedichev *et al.*, *ibid.*, **60**, 3220 (1999).  
[23] D.L. Feder *et al.*, Phys. Rev. A **62**, 053606 (2000).  
[24] A.L. Fetter and A.A. Svidzinsky, J. Phys.: Cond. Matt. **13**, R135 (2001).

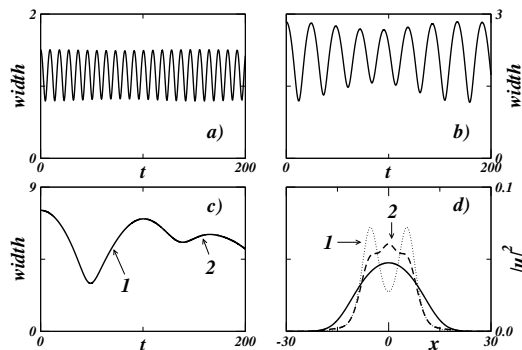


FIG. 1. Condensate width as a function of time for  $\Omega = 0.3$  (a),  $\Omega = 0.1$  (b), and  $\Omega = 0.02$  (c). In (d) we plot the atomic density with  $\Omega = 0.02$  at three different times:  $t = 0$  (solid line),  $t = 80$  (dotted line, corresponding to point 1 in (c)) and  $t = 160$  (dashed line, corresponding to point 2 in (c)).

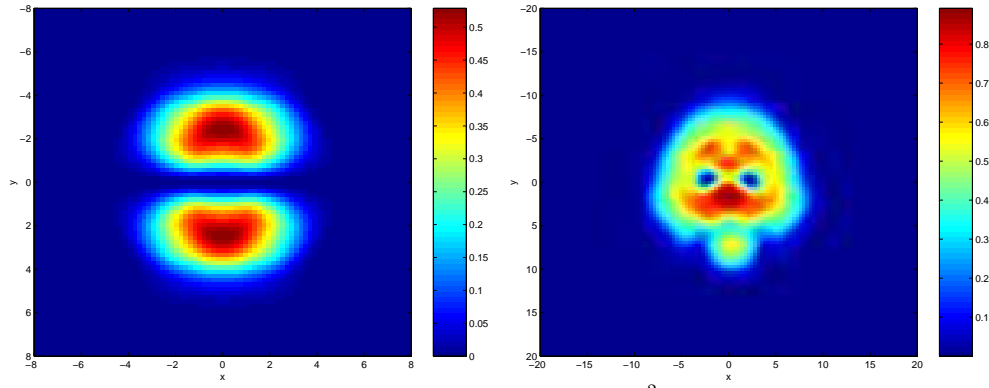


FIG. 2. The panels show the contour plots of the density  $|u|^2$  for  $\Omega = 0.35$  at  $t = 1000$  (left) and  $\Omega = 0.15$  at  $t = 200$  (right). In the first case the transverse instability is clearly suppressed, while in the second it sets in, giving rise to a formation of a vortex pair.

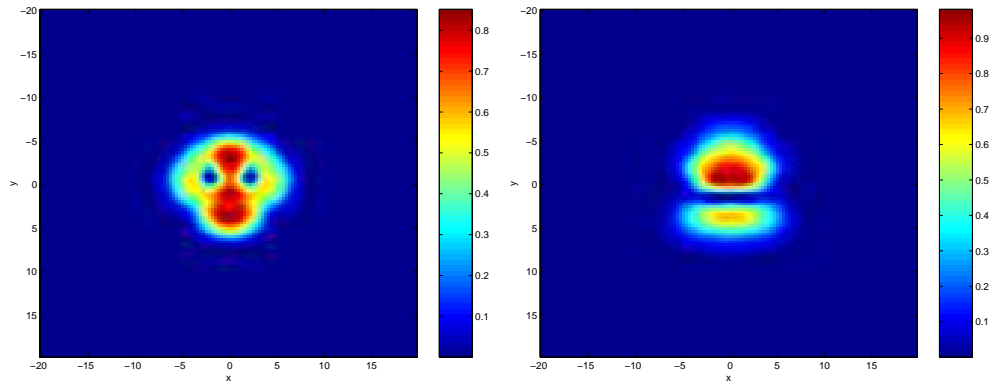


FIG. 3. Snapshots of a vortex-pair evolution in a case where snaking instability has set in ( $\Omega = 0.2$ ). In the left panel ( $t = 190$ ) the formed vortex pair is shown, while the right panel ( $t = 210$ ) shows the recombination of the two vortices, resulting in the re-generation of a dark stripe structure. The latter is unstable and decays at longer times ( $t \approx 400$ ).